
Influence of Wind Velocity Profile on Broadband Noise Emissions from Wind Turbine Blades Under Neutral Atmospheric Conditions

Vasishta Bhargava NUKALA *

Department of mechanical engineering, GITAM (Deemed to be) University Patancheru Hyderabad, Telangana, India, vasishtab@gmail.com

Chinmaya Prasad PADHY

Department of mechanical engineering, GITAM (Deemed to be) University Patancheru Hyderabad, Telangana, India, cppadhy@gitam.edu

* Author to whom correspondence should be addressed

Abstract: - Aerodynamic noise from wind turbines became a prime concern due to demand for wind power. Proper planning regulations must aim at minimizing any deleterious effects of noise on inhabitants near wind farms. Researchers till now have investigated noise from rotating blades of wind turbine with a focus on geometric parameters of blade and little or no research done about the impact of wind velocity profile on broadband noise from large size turbines. This paper investigates the effect of log law and power law wind velocity profile on noise emissions in neutral atmospheric boundary layer conditions. Brooks, Pope & Marcolini and Moriarty & Migliore methods have been implemented for computing turbulent boundary layer trailing edge noise and inflow broadband noise from 2 MW wind turbine. Computational results demonstrate that using power law exponent range of 0.05-0.2, inflow noise increased by 2-5 dB for entire frequency spectra while trailing edge noise increased by 2 dB for frequency below 1 kHz. With log-law profile, the trailing edge noise showed a change of 10 dB while for inflow noise showed a change up to 5 dB when roughness varied from 0.01 to 0.1. The overall noise predicted by both methods using power and log law have been validated with measured data of GE 1.5sle and Siemens SWT turbines at wind speed of 11 m/s. It was found that overall noise obtained using power law agreed with experiment data within 2 dBA while log-law predictions deviate by 4-7 dBA for frequency below 1 kHz and within 1 dBA for frequency higher than 1 kHz.

Keywords: - wind turbine, sound pressure, wind shear, wind speed, noise, power law, log law.

1. INTRODUCTION

In the recent times, research on wind turbine noise emissions has extensively progressed due to its significant effects on long term public health living near the wind farms. As wind power plants continue to grow at a faster rate due to advancement of manufacturing technologies, turbines size with longer blades and higher tip speed has the potential to produce higher noise emissions in surrounding areas. Even though noise exposure from aircraft and road traffic dominate community noise levels, perception and annoyance of wind turbine noise among inhabitants is high and becomes stronger due to non-acoustical factors (e.g. time of day or night) during specific environmental conditions. Therefore, use of noise evaluation criteria based on perception and annoyance are required during design and assessment of wind turbine systems for social acceptance. Wind turbines operate in surface atmospheric boundary layer conditions in which temperature effects such as inversion and lapse influence changes to the turbulence intensity and wind shear experienced by the neighboring turbines in the wind park leading to

lowering power production and increased noise emissions. In the past, several researchers have proposed semi-empirical methods for predicting airfoil self-noise mechanisms from airfoils and wind turbine blades. In case of wind turbine blades, two important aerodynamic noise sources are airfoil self-noise from rotating blades and turbulent inflow noise from blades due to atmospheric turbulence patterns. The validation methodology implemented by [1] was based on rapid distortion anisotropic turbulent velocity spectrum for predicting turbulent inflow noise from thin airfoils. Fig. 1 shows a typical topographic structure of a land-based wind turbine and its influence on the velocity profiles experienced by turbines. The stability pattern of velocity profiles within boundary layer is essential to estimate not only the mechanical and aerodynamic loads on the turbine but also to predict the acoustic emissions. [2,3] studied the influence of atmospheric stability patterns on the measured sound pressure levels from utility scale wind farms located in Netherlands and found that noise data collected during day, evening and night times varied by a difference of 5dB. A further investigation on microphone screen induced noise

and background noise levels from the field measurements was conducted to verify the influence of microphone screen diameter and location on measured sound pressure level. Numerous studies on noise emissions from wind turbines have been conducted to find the potential sources of airfoil self-noise as well as from the interaction of moving blades with tower wake flow in various operating conditions. Particularly, [4,5] suggested semi empirical methods for trailing edge and inflow turbulence noise emissions applicable for helicopters, wind turbines and propellers. However, improved inflow and trailing edge methods were developed by [6,7] based on the quasi-empirical expressions to the sound pressure level. These methods were initially derived for thin airfoils with finite span and varying chord lengths and relied on several assumptions related to turbulent flow parameters which include turbulence intensity, length scale, and boundary layer displacement thickness, flow angle of attack, mean flow velocity to predict sound pressure. The long-range sound propagation effects in atmosphere were done to investigate the noise levels produced from arrays of wind turbines operating in complex terrain conditions. High fidelity and improved noise prediction methods have also been proposed for full scale and prototype wind turbine operation in varied wind shear and atmospheric turbulence conditions [8, 9, 10, 11]. Additionally, fundamental concepts to predict the amplitude modulation of trailing edge aerodynamic noise taken during measurements in a wind farm by [12, 13] are reviewed.

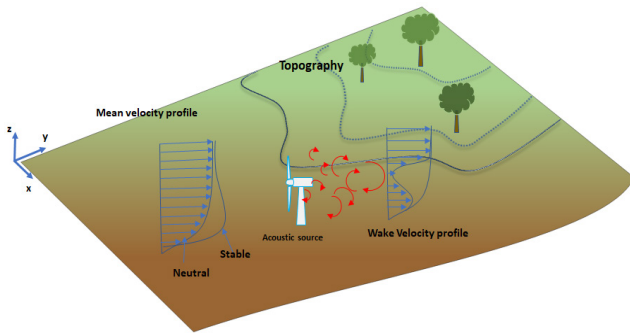


Figure 1 Sketch of wind turbine operating environment in topographic conditions

The influence of blade tower wake interaction on the leading-edge impulsive noise source caused due to unsteady flow over the downwind rotor blades were discussed and active control methods to mitigate the low frequency broadband noise were also proposed. In this paper, the influence of wind velocity profiles on the sound emissions are investigated using methods developed by [6, 7] for a utility scale 2MW wind turbine. Power and log-law profiles are implemented for varying wind shear exponents,

surface roughness lengths (indicative of terrain roughness) at mean hub height velocity of 11 m/s. Results for 1/3rd octave A-weighted overall sound power level (OASPL) are compared for both velocity profiles and compared to measured data of GE-1.5sle and Siemens SWT wind turbines.

2. METHODS

In this section, semi empirical methods proposed by [6, 7] are discussed. These methods can predict the turbulent inflow and trailing edge self-noise from blades utilizing the turbulence velocity spectra and boundary layer properties. Figure 2 illustrates the turbulent inflow and aerodynamic self-noise generation mechanisms from a rotating wind turbine blade. Primary source of noise occurs from trailing edge of blade during operation due to turbulent boundary layer flow on blade surface having finite impedance. This type of noise can vary in intensity depending on flow angle of attack, mean velocity and receiver positions relative to moving source in rotor plane. However, the strength of turbulent inflow noise has been found to be dependent on large scale turbulent eddies size in incoming flow comparable to leading edge curvature of blade. It also varies with turbulence intensity in the atmospheric boundary layer.

2.1 Turbulent inflow noise

The turbulent inflow noise method proposed by [6] has been implemented in the present study. This method uses low frequency directivity factor and characterizes low and high frequency noise levels in the sound power spectra. To include the turbulence characteristics in the noise prediction method, it uses the low frequency correction factor which is derived from the Amiet's experiments on thin airfoil [6]. The acoustic pressure for turbulence induced noise can be evaluated by Eq. (1) to Eq. (4)

$$SPL_{in} = SPL_H + 10 \cdot \log \left[\frac{LFC}{1+LFC} \right] \quad (1)$$

$$SPL_H = 10 \cdot \log \left[\frac{\rho^2 c^2 l L}{2r^2} M^3 u^2 I^2 \frac{K^3}{(1+K^2)^{3/2}} D_L \right] + 78.4 \quad (2)$$

$$LFC = 10S^2 MK^2 \beta^{-2} \quad (3)$$

$$S^2 = \left(\frac{2\pi K}{\beta^2} + \left(1 + 2.4 \frac{K}{\beta^2} \right)^{-1} \right)^{-1} \quad (4)$$

Here, $\beta = \sqrt{1 - M^2}$, $K = \frac{\pi f c}{U}$ and LFC is low frequency correction factor involving the aero-acoustic transfer function, S which varies with acoustic wave number K . L is the span length of

airfoil source, and I is the turbulence intensity, l is the integral length scale parameters and r is the total or effective distance position of microphone from turbine. To take account of compressibility effects of turbulent flows on generation of acoustic field, it also considers the Prandtl-Glauert compressibility criterion as function of Mach number, M and given by β . D_L is the low frequency directivity function expressed in terms of observer angles in the rotor and azimuthal planes respectively.

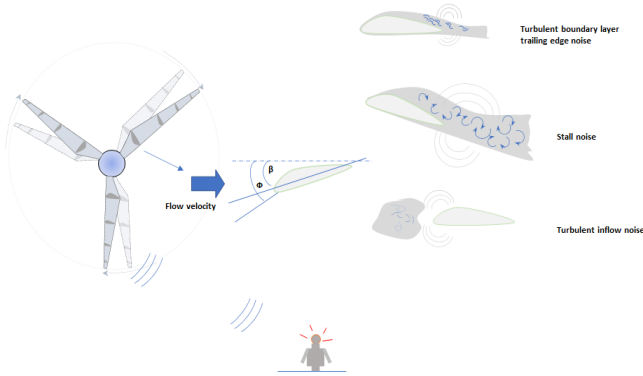


Figure 2 Illustration of types of noise sources from a wind turbine rotor and noise perceived by receiver (adapted from [8])

2.2 Turbulent Boundary Layer-Trailing Edge Noise

Airfoil self-noise mechanisms was investigated by [7] based on wind tunnel experiment data of thin symmetric airfoils with chord length ranging from 2.5 cm to 60 cm. NACA0012 airfoil was chosen and modeled as half infinite flat plate structure. The empirical derived expressions for far field sound pressure level constitute geometry properties of airfoils and boundary layer parameters such as boundary layer thickness, in terms of chord and angle of attack. Also, a directivity function was included to analyze the effect of sound field radiation close to source. Furthermore, in this method, the acoustic pressure is predicted using the logarithmic scaling of boundary layer variables, predominantly displacement thickness δ^* , Mach number M , high frequency directivity function D_h , effective distance between microphone and turbine r_e , blade span length L , and spectral shape functions A and B depend on the Strouhal number, St . Also, the sound pressure levels vary with fifth power of local velocity or free stream Mach number, M^5 and with chord Reynolds number, Re_c . The broadband noise spectrum is divided into three components viz. pressure side component uses directivity and appears dominant in high frequency region, suction side component exhibits noise peak towards low frequency part of the spectrum and the stall noise component is dependent on flow angle and

shows a noise peak in the mid band to high frequency region. Both the sources are found to vary negligibly with angle of attack. The stall separation noise is critical to angle of attack and produces peaks at high positive values of angle of attack. This noise source reduces to compact dipole and uses low frequency directivity function. The flow separation noise also occurs for high positive angle of attack for which high frequency directivity is used. The three noise sources are added logarithmically along the individual blade segments for each blade to obtain resultant overall sound pressure. The empirical equations involved to evaluate the sound pressure is given by Eq. (5) - Eq. (8)

$$SPL_p = 10. \log \left[\frac{\delta_p^* M^5 L D_h}{r_e^2} \right] + A \left[\frac{St_p}{St_1} \right] + [K_1 - 3] + \Delta K_1 \quad (5)$$

$$SPL_s = 10. \log \left[\frac{\delta_s^* M^5 L D_h}{r_e^2} \right] + A \left[\frac{St_s}{St_1} \right] + [K_1 - 3] \quad (6)$$

$$SPL_\alpha = 10. \log \left[\frac{\delta_s^* M^5 L D_h}{r_e^2} \right] + B \left[\frac{St_s}{St_2} \right] + K_2 \quad (7)$$

$$SPL_{Total} = \sum_{i=1}^N 10. \log \left[10^{\frac{SPL_i}{10}} \right] \quad (8)$$

The Strouhal number (St) is used for analyzing the flow induced vibrations in turbulent flows and involves center frequency as well as characteristic dimension of source. For turbulent boundary layer flows over aerofoil it is calculated using pressure and suction side displacement thickness, given by Eq. (9)

$$St = \chi(f, \delta_k^*, U, M) \quad (9)$$

Here, subscript k refers to either the suction and pressure side boundary displacement thickness of aerofoil, δ^* is the boundary layer displacement thickness, f is 1/3rd octave center frequency. For turbulent boundary layer flows over an aerofoil it is calculated using pressure and suction side displacement thickness and given by Eq. (10) and Eq. (11).

$$St_p = \left[\frac{f \delta_p^*}{U} \right] \quad (10)$$

$$St_s = \left[\frac{f \delta_s^*}{U} \right] \quad (11)$$

It can be seen that St_i is related to turbulent boundary layer trailing edge noise and subscripts with p and s refer to pressure and suction side of airfoil. Similarly St_2 is related to evaluate the stall separation noise in spectra [5,7]. This quantity varies significantly with free stream velocity (U) and Mach number (M) and typical values for this quantity vary between 0.01 and 10 for low Mach number flows. The Reynolds number expresses the relation between inertial and viscous forces in a flow field, given by Eq. (12) and Eq. (13). This parameter is function of suction and pressure side displacement thickness and

also chord length of aerofoil which is characteristic dimension. To evaluate frequency dependent level adjustment function, ΔKI , and broadband amplitude functions, $K1$ and $K2$, Reynolds number is evaluated at every $1/3^{\text{rd}}$ octave frequency. For wind turbines the blade typically experiences moderate to high Reynolds number of order 3.5×10^6 for turbulent flows and vary along its length. This type of source uses high and low frequency directivity functions, given by Eq. (14) and Eq. (15)

$$Re_p = \left[\frac{\delta_p^* U}{\vartheta} \right] \quad (12)$$

$$Re_c = \left[\frac{Uc}{\vartheta} \right] \quad (13)$$

$$D_H(\theta, \varnothing) = \frac{2 \sin^2(\frac{1}{2}\theta) \sin^2(\varnothing)}{(1+M \cos\theta) \cdot (1+(M-M_c) \cos\theta)^2} \quad (14)$$

$$D_L(\theta, \varnothing) = \frac{\sin^2(\theta) \sin^2(\varnothing)}{(1+M \cos\theta)^4} \quad (15)$$

The boundary layer thickness (δ) and displacement thickness (δ^*) are calculated as function of the chord length of aerofoil (c) and angle of attack for both pressure and suction sides of aerofoil, as given in [7]. For this type of source, the acoustic pressure produced near trailing edge varies as fifth power of Mach number dependence or M^5 and exhibits cardioid pattern of noise radiation at trailing edge. However, this pattern can vary with intensity of mean velocity and source boundary conditions. Further, for low Mach number flows, $M \sim 0.2$, noise radiated from pressure and suction sides of aerofoil depend upon the spectral functions A and B , which are correlated with the aerodynamic and boundary layer properties [5, 7]. The spectral function A is related to turbulent boundary layer-trailing edge noise and function B with flow separation noise. For non-compact sources and attached flows, high frequency directivity function (D_H) is used and given by $\sin^2(\frac{\theta}{2})$ to predict trailing edge noise. The convective nature of acoustic pressure waves can be described by $(1 + M \cos\theta) [1 + (M - M_c \cos\theta)]^2$ terms. For stalled or fully separated flow on blade, the trailing edge noise source can reduce to a dipole pattern and varies as M^6 . Therefore, for such case, angles of attack usually exceed 12.5° for which low frequency directivity, D_L is also used. The directivity angles, θ and \varnothing , are aligned in the azimuth and polar directions of rotor plane for turbine.

The log-law and power law for wind velocity profiles have been defined by Eq. (16) and Eq. (17) [14].

$$\frac{U(z)}{U(z_r)} = \ln \left(\frac{z/z_0}{z_r/z_0} \right) \quad (16)$$

$$\frac{U(z)}{U(z_r)} = \left(\frac{z}{z_r} \right)^\alpha \quad (17)$$

Here, z is the surface roughness height in m. z_0 is the standard or reference roughness height, z_r is the roughness height at r m above the ground. U is the mean wind velocity at given height in m/s, α is the wind shear exponent.

3. RESULTS

Table 1 shows the turbine specifications for assessment of overall sound power level. The [6, 7] noise methods have been simulated using MATLAB software. The turbine parameters are given as key inputs to blade element momentum method to evaluate aerodynamic flow field data and coupled to noise solver for prediction of noise. The receiver (microphone) distance is fixed at 120 m downwind direction from source and at height of 0.2 m above ground.

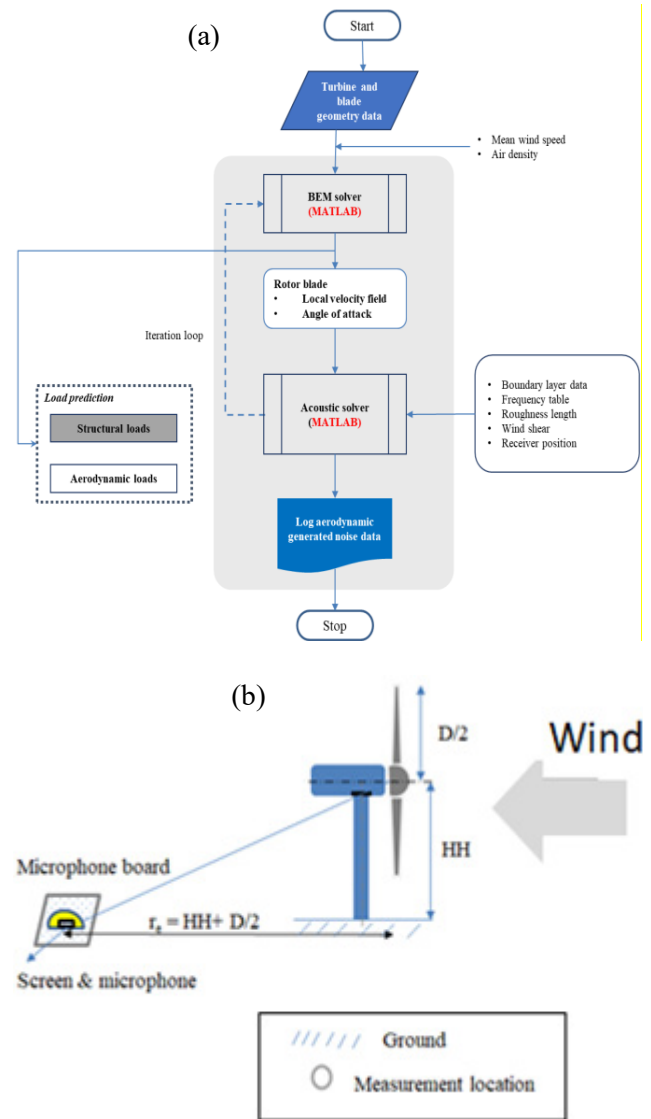


Figure 3 (a) Schematic of computational routine for predicting trailing edge and turbulent inflow noise (b) Diagram of microphone location for measurement according to IEC 61400-11 acoustic emissions [16]

Figure 3(a) shows the illustration of computational procedure followed for implementing the turbulent boundary layer trailing edge noise and turbulent inflow noise. Figure 3(b) demonstrates the placement of microphone position according to IEC-61400-11 standard for acoustic emission measurements.

It must be noted that the atmospheric propagation effects such as absorption (from air or ground), scattering and refraction (caused due to wind and temperature gradients) around obstacles are not considered in semi-empirical methods. To account for these effects on assessment of overall sound power, IEC 61400-11 standard for acoustic emission measurements criteria has been considered which deducts 6 dB for the attenuation of sound due to the above factors. Geometric spherical spreading has been included in noise simulation and considers blade as dipole point source

Figure 4 illustrates the velocity profiles as function of height above ground computed using log-law and power law at free stream velocity of 11 m/s at shear exponent of 0.1 and roughness length of 0.05 (representative of plain grass land).

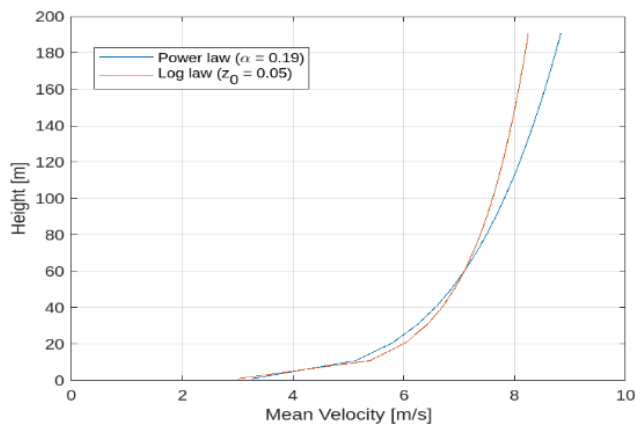


Figure 4 Comparison of wind velocity profile obtained from power and log law distributions at mean wind speed of 11 m/s using wind shear exponent (α) of 0.1 and surface roughness (z_0) of 0.05m

Fig 5(a) and Fig 5(b) demonstrates the comparison of 1/3rd octave frequency spectra of turbulent inflow noise computed using method from [6] and by implementing log-law and power law wind velocity profiles.

On the other hand, for increasing wind shear exponent, the change in sound power values is found significant for frequencies, $f < 1$ kHz.

For high frequencies, $f > 1$ kHz, the changes to sound power values remain insignificant. It can be noted that trailing edge noise is produced significantly from rotor blades during the downwind direction of rotation in rotor plane

[4,5,6,10,12,15,16,17]. This broadband phenomenon is perceived as *swish* by observer in rotor plane and propagates in far field as result of amplitude modulation of sound waves at blade passing frequencies.

Fig. 6(a) and Fig 6(b) illustrates the trailing edge noise computed using the method developed by [7] at mean wind speed of 11 m/s. A comparison of results from log-law and power law profiles for wind shear reveals that effect of roughness on trailing edge noise from blades influences the sound power by 4-6 dBA.

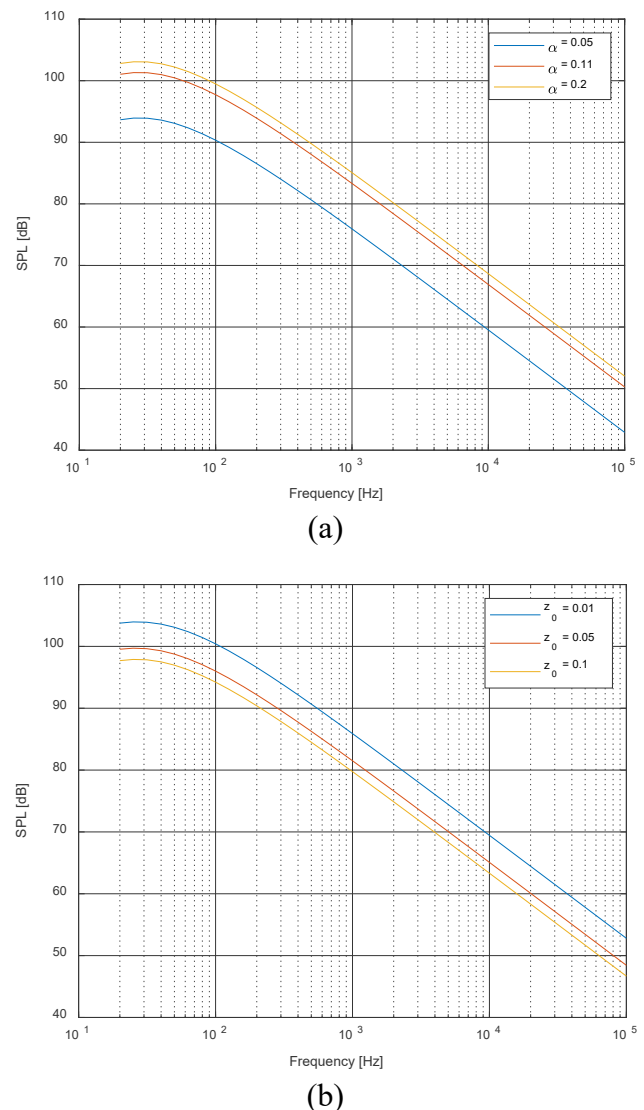


Figure 5. Comparison of turbulent inflow noise from a 2 MW wind turbine: (a) for different wind shear exponents using power law; (b) for different roughness values using log law

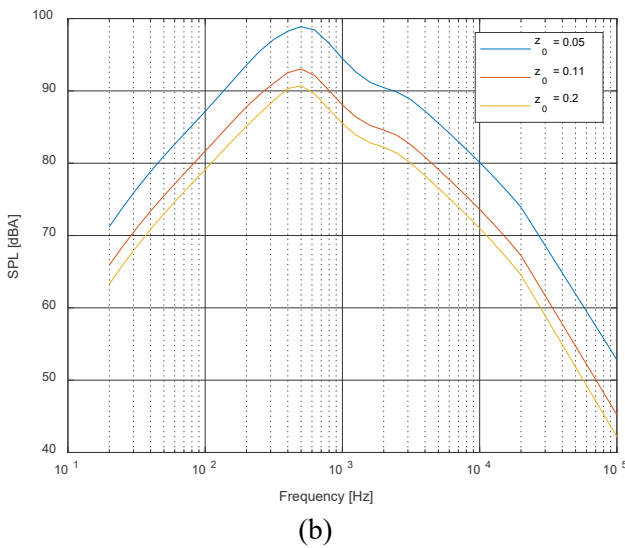
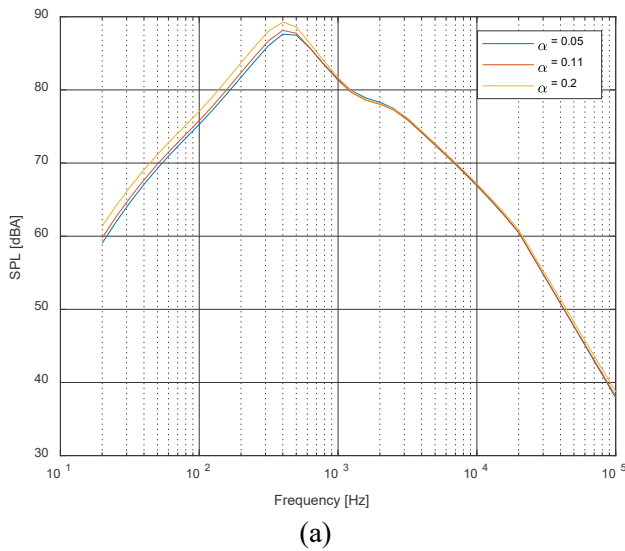


Figure 6. Comparison of turbulent boundary layer trailing edge noise for 2 MW machine (a) for different wind shear exponents using power law (b) for different surface roughness values using log law

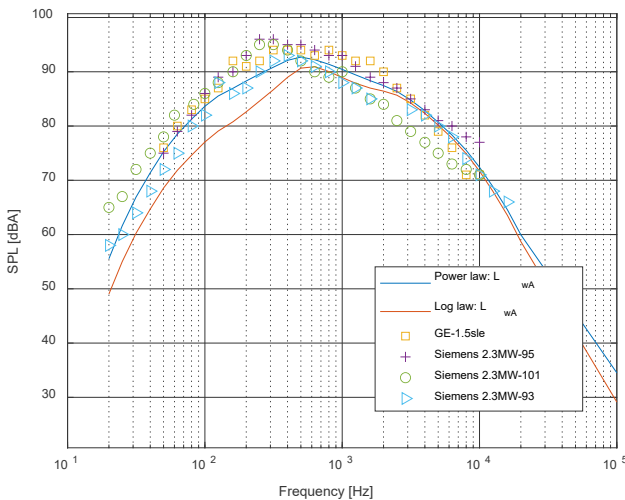


Figure 7. Comparison of overall A-weighted sound power from a 2MW machine obtained using power law and log law distribution with measured data of GE-1.5sle, Siemens 2.3MW 95, Siemens 2.3MW 101 and Siemens 2.3MW 93 turbines.

Figure 7 shows the validation of overall sound power level considering the broadband turbulent inflow and trailing edge noise components.

Table 1. Design variables for 2 Megawatt turbine

Parameter	Value
Cone	0°
Tilt	~3°
Tower height	~80 m
Length of blade	~37 m
Rotor speed	~17 RPM
Maximum twist	~13°
Maximum chord	~3.22 m
Orientation	upwind
No of blades	Three
Rated power	2 Megawatt

4. CONCLUSIONS & FUTURE WORK

The present study investigated the effect of wind velocity profiles using power and log-law on broadband noise generation for 2MW wind turbine in neutral atmospheric condition. The turbulent inflow noise method results have shown that when both wind shear exponents, roughness lengths are varied from a range 0.01 to 0.2, sound power was found to increase by ~2-8dB keeping other factors constant. The method for turbulent boundary layer trailing edge noise developed by [7] is a good predictor in the high frequency region of noise spectra and showed good agreement with experiment data. Both methods have demonstrated good accuracy for predicting overall sound power level however, wind velocity profile based on power law agreed remarkably well with experiment data than log law profile in low frequency region of noise spectrum and thus more realistic. The stability of atmospheric turbulence in the boundary layer and its influence on sound power from wind turbines can be investigated further.

ACKNOWLEDGMENTS

This research was supported by GITAM (Deemed to be) University and authors would like to thank them for the computational facilities provided during this process.

REFERENCES

[1] Faria, M. A., Saab Jr, J. Y., Rodriguez. S., Pimenta M.M., A rapid distortion theory based aerofoil turbulent inflow noise prediction method, *Journal of Brazilian society of mechanical sciences and engineering*, Vol 42, No 397, 2020, pp 1-9

-
-
- [2] Van den Berg, The sound of high winds: effect of atmospheric stability on wind turbine sound and microphone noise, Doctoral Thesis, University of Groningen, Netherlands, (2006)
- [3] Van den Berg, Wind turbine noise: an overview of acoustical performance and effects on residence, *Proceedings of acoustics*, Victor harbor, Australia (2013)
- [4] Hubbard, H.H., Shephard, K.P., Aeroacoustics of large wind turbines, *Journal of acoustical society of America*, 6(89), pp. 2495 – 2508 (1991)
- [5] Grosveld, F.W., Prediction of Broadband Noise from Horizontal Axis Wind Turbines, *Journal of Propulsion and Power*, 4(1), pp. 292-299, (1985)
- [6] Moriarty, P., Migliore, P., Semi Empirical Aero-Acoustic Noise Prediction Code for Wind Turbines [Technical report], (2003) Available from: <http://citeseerx.ist.psu.edu/viewdoc/download?doi=10.1.1.197.1153&rep=rep1&type=pdf>
- [7] Brooks, T.F., Pope, D.S., Marcolini, M.A., Airfoil Self Noise and Prediction. NASA reference publication 1218, (1989) Available from: <https://ntrs.nasa.gov/archive/nasa/casi.ntrs.nasa.gov/19890016302.pdf>
- [8] Shen, W. Z., Zhu, W.Z., Barlas, E., Li, Y., Advanced flow, and noise simulation method for wind farm assessment in complex terrain, *Journal of Renewable Energy*, (143), pp 1812-1825, (2019), <https://doi.org/10.1016/j.renene.2019.05.140>
- [9] Cotte, B., Tian, Y., Wind turbine noise modeling based on Amiet's theory: Effects of wind shear and atmospheric turbulence, *Acta Acustica united with Acustica*, 4(102), pp. 626-639, (2016)
- [10] Oerlemans, S., Lopez, M. B., Acoustics array measurements on a full-scale wind turbine, *11th AIAA / CEAS aeroacoustics conference*, Monterey, California, (2005), <https://doi.org/10.2514/6.2005-2963>
- [11] Dragn, D., Emmanuelli. A., Colas, J., Stevens, R.J.A.M., Blanc-Benon. P., (2022) Effect of a 2D hill on the propagation of wind turbine noise, *AIAA*, Vol 2923, (2022), <https://doi.org/10.2514/6.2022-2923>
- [12] Doolan, C., Moreau, D.J., Arcondoulis, E., Albarracin, C., Trailing Edge Noise Production, Prediction and Control. *New Zealand Acoustics*, 3(25), pp. 22-29, (2012)
- [13] Bresciani, A.P.C., Maillard, J., De Santana, L.D., Perceptual evaluation of wind turbine noise, *16th congress francais d' Acoustique*, Marseille, France, (2022)
- [14] Ray, M.L., Rogers, Al.L., McGowan, J.G., Analysis of wind shear models and trends in different terrains, *Renewable energy research laboratory*, University of Massachusetts, Amherst, USA (2014)
- [15] Merino-Martinez, R., Pieren, R., Schaffer, B., Holistic approach to wind turbine noise: From blade trailing edge modifications to annoyance estimation, *Renewable and sustainable energy reviews*, 148, (2021), <https://doi.org/10.1016/j.rser.2021.111285>
- [16] Bhargava, V., Samala, R., Effect of boundary layer and rotor speed on broadband noise from wind turbines, *Journal of aerospace technology and management*, <https://doi.org/10.5028/jatm.v11.1045>, (2019)
- [17] Bhargava, V., Kasuba, S., Maddula, S.P., Jagadish, D., Khan, Md. A., Padhy, C. P., Chinta, H.P., Chekuri, C.S.V., Dwivedi, Y.D., A case study of wind turbine loads and performance using steady-state analysis of BEM, *International journal of sustainable energy*, (2020) <https://doi.org/10.1080/14786451.2020.1787411>